

# Sag-tension evaluation of high-temperature gap-type conductor in operation

Miren T. Bedialauneta<sup>1</sup>  | Elvira Fernandez<sup>2</sup>  | Igor Albizu<sup>1</sup>  | A. Javier Mazon<sup>2</sup> 

<sup>1</sup> Dept. of Electrical Engineering, University of the Basque Country UPV/EHU, Faculty of Engineering Gipuzkoa, Otaola Etorbidea 29, Eibar, Spain

<sup>2</sup> Dept. of Electrical Engineering, University of the Basque Country UPV/EHU, Faculty of Engineering Bilbao, Alameda Urquijo s/n, Bilbao, Spain

## Correspondence

Miren T. Bedialauneta, Dept. of Electrical Engineering, University of the Basque Country UPV/EHU, Faculty of Engineering Gipuzkoa, Otaola Etorbidea 29, 20600, Eibar, Spain.  
Email: [miren.bedialauneta@ehu.eus](mailto:miren.bedialauneta@ehu.eus)

## Funding information

Ministerio de Economía, Industria y Competitividad, Grant/Award Number: DPI2016-77215-R; University of the Basque Country, Grant/Award Number: ELEKTRIKER research group GIU20/034

## Abstract

Low-sag conductors are characterised by their ability to operate above the “knee-point temperature” (KPT). Sag-tension performance must be calculated while designing a new overhead line. The ampacity limit of the conductor is influenced by the sag and the temperature of the conductor. The maximum sag must be limited to a certain value to ensure a safe clearance between the conductor and ground. In this study, a gap-type conductor in operation was monitored to evaluate the actual KPT. The KPT in low-sag conductors is a crucial factor since it affects the sag of the conductor, which must be limited for safety reasons. The KPT was detected based on the change in the coefficient of thermal expansion value of the conductor. To perform this detection, the conductor tension and temperature were monitored. This study proposes a procedure to estimate the coefficient of thermal expansion (CTE) value. The results showed a gradual displacement in CTE. This procedure was used to perform measurements in a pilot line.

## 1 | INTRODUCTION

The demand for electricity has grown exponentially in recent times. This demand is set to increase with the integration of electric vehicles and the development of newer technologies that require electricity for their operation. To supply this growing electricity demand, the power flow in electrical lines has increased considerably.

As a result of this increased power flow, the current carrying limit of some lines can reach their ampacity limit. The ampacity of a conductor is the maximum constant current that the conductor can carry, according to the design, security, and safety criteria of a line made from that conductor [1].

In addition, the advent of renewable generation such as wind and photovoltaic plants has led to changes in the power flow in transmission systems. This is because these plants are usually located at a certain distance from the loads they supply. As a result, some existing overhead transmission line circuits are required to handle considerably higher and increasingly variable power flows than their original ampacity (thermal rating) during normal, emergency, and post-contingency states [1].

The ampacity limit of a conductor is related to the operating temperature and sag of the conductor. The difference in the level between points of supports and the lowest point on the conductor is called sag. In the case of overhead lines, the maximum sag must be limited to a certain value to ensure sufficient clearance between the conductor and ground. An increase in the sag ( $A$  as shown in Figure 1) results in a decrease in the ground clearance and vice versa. For safety reasons, the ground clearance must be kept to the permissible minimum electrical clearance. This is referred to as the safety clearance between the conductor and the ground at maximum permissible sag ( $B$  as shown in Figure 1). A high conductor temperature causes excessive elongation of the conductor, which consequently results in a dangerous reduction of the ground clearance ( $C$  as shown in Figure 1). The maximum temperature of the conductor is related to the maximum value of the sag.

Sag determination is to obtain a safe distance of the object below the overhead conductor and to determine the conductor length and tower height [2–5]. Several studies on sag and safety distance have been undertaken [6–11]. In [6] the method of calculating sag with the effect of conductor weight, tensile

This is an open access article under the terms of the [Creative Commons Attribution](https://creativecommons.org/licenses/by/4.0/) License, which permits use, distribution and reproduction in any medium, provided the original work is properly cited.

© 2021 The Authors. *IET Generation, Transmission & Distribution* published by John Wiley & Sons Ltd on behalf of The Institution of Engineering and Technology

strength, span distance, elevation angle between two towers, temperature and wind is presented. Safety distance. Transmission line simulation method to detect safety distance is developed by combining the influence of weather conditions, and the verification of these results using laser scanning data is described in [7]. The sag is measured by using a line inspection robot in [8]. In [9–11] the authors apply simulation or finite element modelling methods to calculate the sag or safety distance.

Replacing the existing conductors with high-temperature low-sag (HTLS) conductors presents a safe and secure way to increase the power flow in the line without the need to strengthen the towers [1, 12, 13]. These conductors operate at higher temperatures than that those required for conventional conductors, and their coefficients of thermal expansion (CTEs) are lower than those of conventional conductors. Low-sag conductors are characterised by their behaviour above the temperature referred to as the “knee-point temperature” (KPT). At the KPT, the aluminium is slack, and only the core is under tension. Above the KPT, the rate of sag increase due to temperature rise is lower than that below KPT. The determination of the KPT is a significant factor in evaluating line uprating methods. Therefore, the KPT in low-sag conductors is a crucial factor since it affects the sag of the conductor, which must be limited for safety reasons.

The manufacture and development of various types of HTLS conductors have increased recently [1]. New designs and materials, primarily based on composite materials, have been developed for the conductor core. Among the different types of HTLS conductors, one of the most widely used is the gap-type conductor, which consists of a steel core and aluminium outer strands. A gap that exists between the steel and aluminium layers ensures that the aluminium layers remain slack during the conductor installation process [14].

In the installation methodology [14] of gap-type conductors, the aluminium is left slack during the installation of the conductor; therefore, the KPT of the conductor is considered the installation temperature. As a result, the gap-type conductor works similar to a low-sag conductor above the installation temperature. During its initial sagging condition, mechanical stress is applied only to the steel core. Above the KPT, the aluminium layers are slack (no tension), and the KPT corresponds to the sagging temperature. Therefore, above the KPT, the CTE values of the conductor correspond to those of the steel core. In the case of an aluminium conductor steel-reinforced (ACSR) conductor, the CTE value is almost twice that of a gap-type conductor since the aluminium wires contribute to the rise in CTE [15]. The performance of the conductors is evaluated through laboratory tests [16]. However, to estimate the transition in the KPT, a test has to be conducted with the conductors installed in an actual size span. In some outdoor laboratories, the conductors are installed in real size spans. The conductor temperature is increased by controlling the current in the conductor, and the relation between the sag and temperature is verified.

However, utilities may want to verify the conductor performance in actual operating lines. Occasionally, these utilities install monitoring systems to carry out this verification. At other times, the utilities install monitoring systems to perform

dynamic line rating (DLR), and the information provided by the sensors can be used to evaluate the sag performance of the conductor.

In this study, we explain a case in which DLR monitoring systems are used to evaluate the low sag-tension performance of a GTACSR HTLS conductor in a line in operation. The CTE is estimated through a procedure that compares the theoretical CTE values of the conductor with those obtained from measurements. As a result, the KPT of the conductor is estimated.

In Section 2, the sag-tension calculation of overhead conductors is discussed and the concept of knee-point is described in detail. In Section 3, the pilot line is presented. The measurements and the data processing carried out to minimise the dispersion are described. Besides, the uncertainties in the sag-tension calculation model are discussed and the measures implemented to overcome them are cited. In Section 4, a novel CTE evaluation methodology proposed by the authors is presented. The CTE is estimated for temperature intervals of 10 °C, in steps of 1 °C, and the change in CTE is observed to evaluate the KPT. In Section 5, the results obtained from the application of the method described in Section 4 to the measurements described in Section 3 are presented. Finally, in Section 6, the conclusions are described.

## 2 | SAG-TENSION CALCULATION OF OVERHEAD CONDUCTORS

Sag-tension calculation methods calculate the change in the core and the aluminium tension as a function of temperature. When the temperature increases, the tension in aluminium is transferred to the core since aluminium has a higher CTE value. To predict the sag-tension behaviour in a conductor, the CTE must be known. In non-homogeneous conductors, the sag-tension behaviour is distributed in two sections: below the KPT and above the KPT. In other words, these sections are above and below the temperature at which aluminium ceases to support the conductor load. Two CTE values, one below the KPT and the other above the KPT, can be measured, and these values must agree with the typical values [16, 17].

The maximum sag in overhead lines must be limited to a certain value to ensure sufficient ground clearance. When the temperature increases, the conductor undergoes thermal expansion, which increases the sag. For this reason, the maximum allowable temperature must be limited. Moreover, the sag increases further because of creep, which is the permanent deformation of the conductor. Sag-tension calculation methods calculate the change in the conductor sag as a function of the conductor temperature and time [2–5, 18–20].

While evaluating the sag-temperature performance of overhead conductors using various tests and studies, it is usual to measure KPT values that are higher than expected values. The slope change is observed not where the sag-tension calculation methods define it but at a higher temperature [20].

Various explanations for the higher KPT values have been provided in relevant literature. Nigol and Barrett [21, 22] describe the hypothesis of compression of aluminium at the

KPT: compressive loading of aluminium strands occurs because of the radial movements of the different aluminium layers. The compressive forces on the constrained aluminium strands in a conductor were estimated to vary between 10 and 15 MPa [22]. A few years later, Rawlins proposed an alternative hypothesis describing the effect of conductor manufacturing on the KPT. The hypothesis considered a residual tension during conductor manufacturing and established this tension as the reason for the increase in the KPT [23]. In [24], it is determined analytically and after several laboratory tests that the difference between the temperature during manufacture and the temperature during the installation of the conductor produces an increase in the KPT as well as a difference between the expected KPT and the actual one [24]. The difference between the actual and expected KPTs is justified with the theory of the compression tensions in the outer layers of aluminium. The authors determined that these tensions affected the KPT, and they developed a model taking these tensions into account.

In [4], the authors studied the influence of aluminium compression force and residual aluminium layer stress on the experimental plastic elongation (EPE) model, which models the mechanical and thermal behaviour of the aluminium layers and the steel core separately. Furthermore, the authors concluded that the residual stress in aluminium must be assumed between 15 and 20 MPa for high-temperature sag calculations using the EPE conductor model.

Currently, commercial sag-tension calculation software programs such as the PLS-CADD [25] and SAG10 [26] have the option to consider the compressive stress in aluminium.

In the case of gap-type conductors, the KPT will be the installation temperature and the aluminium is expected to be slack. However, the KPT could be at a higher temperature. As described earlier, there may be compressive forces in the aluminium that increase the temperature at which CTE changes. The KPT is also affected by any residual tension present in aluminium because of the installation process.

The mechanical calculation of the conductor is based on the tension to be supported by the conductor and the sag. The tension is calculated to ensure that the conductor does not exceed its tension limit. The sag is calculated to maintain the safety distances.

Tension-temperature calculation is based on finding the tension  $T$  and the length  $L$  values that satisfy span geometry and conductor behaviour. The conductor characteristics will affect the tension-temperature calculation and, similarly, this will be reflected in the conductor behaviour.

At a certain tension and temperature, the length of the conductor starting from its reference length, varies. The variation in the conductor temperature and tension affects the length of the conductor. In addition, the conductor length increases permanently due to creep. Creep can be defined as the permanent deformation of conductors due to the metallurgical deformation of the conductor material and the geometrical settlement of the conductor wires [27, 28]. The value of creep increases over time. All these changes depend on the conductor characteristics such as manufacturing material, expansion coefficient, and elastic modulus.

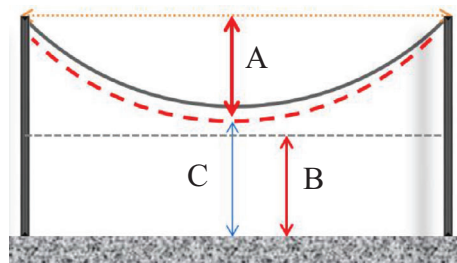


FIGURE 1 Sag and clearance between the conductor and ground



FIGURE 2 Installation of the GTACSR conductor

The thermal expansion due to temperature changes, the elastic deformation produced by tension and the creep or permanent deformation must be considered while investigating the changes in conductor length. The thermal expansion of a conductor is the tendency of the conductor to expand and contract owing to changes in conductor temperature. All tension-temperature calculation methods consider elastic deformation and thermal expansion. However, creep is not considered in every method. Moreover, a large difference is observed in the results between the methods that consider creep and those which do not [2].

### 3 | OPERATING LINE WITH GTACSR CONDUCTOR

A monitoring system was installed on a GTACSR conductor distribution line of 30 kV. This conductor was installed for the purpose of line uprating. The installation of the conductors and the monitoring system was carried out in October 2012 (Figure 2). The length of the monitored span was 282 m.

When a gap-type conductor is installed, the aluminium is left slack; therefore, the KPT is considered as the installation temperature. Further, the conductor shows low sag performance above this temperature. Figure 3 shows two gap-type conductors that were installed. The conductors were installed on different days, and the installation temperatures were 7 and 20 °C for conductors 1 and 2, respectively.

A load cell (Figure 4a) measures the tension in the conductor, and a temperature monitoring system measures the conductor surface temperature (Figure 4b). A weather monitoring system

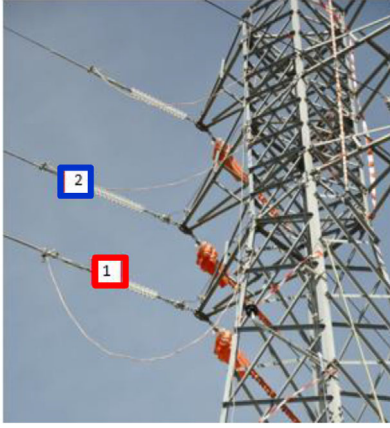


FIGURE 3 Monitored conductors

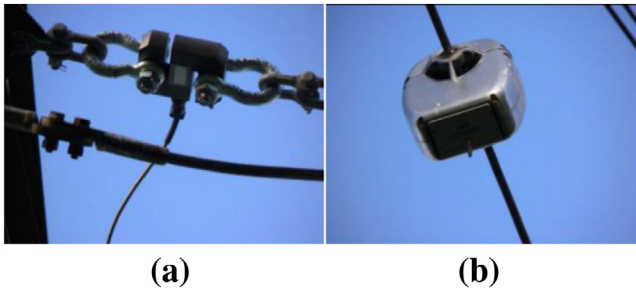


FIGURE 4 Monitoring system. (a) Load cell, (b) Sensor for measuring the conductor surface temperature

was also installed. Measurements were obtained every minute for three years.

The data obtained using the monitoring system are shown in Figure 5.

The measured data detected some dispersion due to tension variations.

### 3.1 | Data processing

Data processing was carried out to minimise the dispersion observed in the measured data. The measured data must satisfy

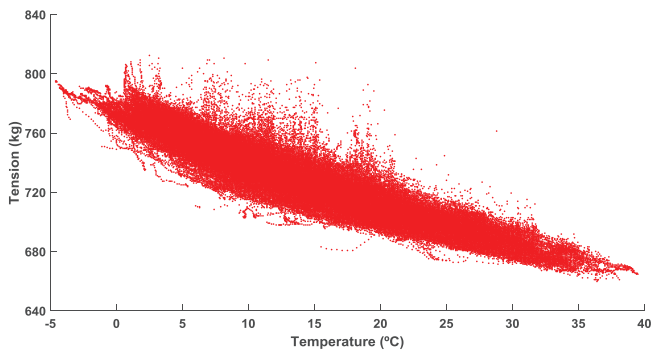


FIGURE 5 Measured tension-temperature values of conductor 1

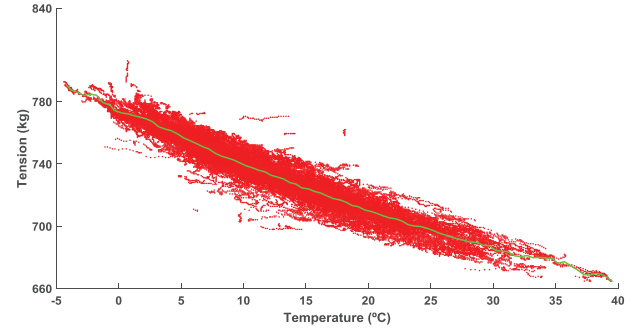


FIGURE 6 Measured data of tension-temperature values and data average (continuous line) of conductor 1

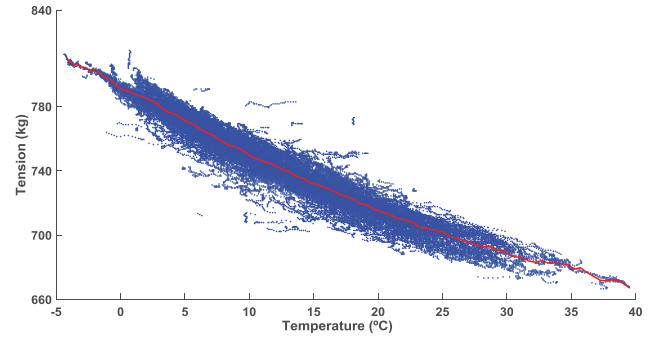


FIGURE 7 Measured data of tension-temperature values and data average (continuous line) of conductor 2

two conditions: First, the difference between the tension values of two consecutive data must not exceed 1 kg; finally, the number of data that satisfy the first condition must be at least ten. As observed from Figures 6 and 7, the dispersion was minimised upon imposing these conditions on the measured data. To obtain uniform distribution, the averages of the data were calculated and these values were plotted (continuous line) on the graphs obtained after data processing.

### 3.2 | Theoretical model

The theoretical model used for the sag-tension calculation is defined by Equations (1) and (2). The parameters included in the sag-tension model are the span length  $a$ , conductor weight  $\omega_{\text{con}}$ , elastic modulus  $E$ , area  $A$ , and coefficient of thermal expansion  $CTE$ .

$$L_{\text{cat}} = 2 \cdot \frac{T}{\omega} \cdot \sinh\left(\frac{a \cdot \omega}{2 \cdot T}\right). \quad (1)$$

$$L_{\text{con}} = L_0 \cdot \left[ 1 + CTE \cdot (\theta - \theta_0) + \frac{T - T_0}{E \cdot A} \right]. \quad (2)$$

The conductor tension  $T$  is iterated for each conductor temperature  $\theta$  until the values of catenary length  $L_{\text{cat}}$  and

the conductor length  $L_{\text{con}}$  are equal. The total load in the conductor  $\omega$  is the same as the conductor weight  $\omega_{\text{con}}$  if there is no overload.  $L_o$  is the reference length of the conductor at a certain temperature  $\theta_o$  and tension  $T_o$ .

The equivalent *CTE* (*CTE* of the conductor) depends on the *CTEs* ( $CTE_c$  and  $CTE_a$ ), moduli of elasticity ( $E_c$  and  $E_a$ ), and the sections ( $A_c$  and  $A_a$ ) as expressed in Equation (3), where the subscripts  $a$  and  $c$  refer to aluminium and core, respectively [18, 21].

$$CTE = \frac{E_a A_a CTE_a + E_c A_c CTE_c}{E_a A_a + E_c A_c}. \quad (3)$$

### 3.3 | Minimisation of uncertainty in the calculation model

In the proposed methodology, the theoretical results of the tension-temperature model of the conductor is adjusted with the measured values.

An error in the characteristic parameters of the conductor would affect the calculation, and this error would be reflected in the obtained *CTE*.

For example, an error in the span length or the conductor weight can result in a deviation in the tension-temperature performance that could be wrongly attributed to the low sag characteristic of the conductor if these errors are not considered. Therefore, the factors that affect the tension-temperature performance must be identified, and their influence on the performance must be quantified [29, 30].

To reduce uncertainty, potential errors were considered and the measures implemented to overcome them are listed below:

- It was ensured that the error in the linear mass of the conductor did not exceed 2% [31–33]. The mass of the conductor was verified, and it was found that the mass of the conductor, based on the installed conductor details provided by the manufacturer, did not exceed 0.5% of the nominal mass. This minimises the possibility of error due to the mass of the conductor.
- The elastic modulus of the conductor was verified by the manufacturer by conducting stress-strain tests, and the variation of the elastic modulus, according to the provided data, was limited to 5%.
- A long span (282 m) was chosen for the installation of the monitoring system, thus minimising the possible uncertainty due to short spans. Moreover, the span length was verified by a topographic study.

## 4 | CTE EVALUATION METHODOLOGY

Low-sag conductors are characterised by their ability to operate above the KPT. A change in slope is observed in the sag-temperature behaviour at this temperature. The slope decreases above the KPT because the *CTE* of aluminium is greater than that of the core.

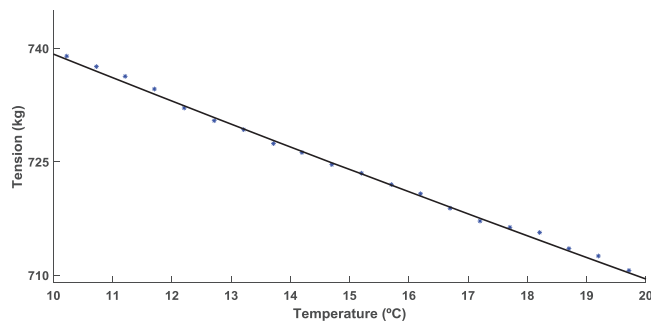


**FIGURE 8** Actual curve (blue points) and theoretical curve (black line) plotted using the *CTE* values obtained for conductor 1

The authors propose a method to quantify the KPT from a continuous evaluation of the *CTE* along the temperature range of the measurements. The method is described in this section. There is a lack of methods with the objective to determine the KPT in a systematic way, and the proposed method fills this gap.

The error in *CTE* is the difference between the *CTE* obtained through actual measurements (actual *CTE*) and the *CTE* provided by the manufacturer (theoretical *CTE*). Upon evaluating the actual *CTE*, the KPT at which the aluminium gets slack can be calculated.

The *CTE* can be estimated by minimising the mean squared error between the calculated and measured tension values. Moreover, the *CTE* is estimated based on temperatures. Additionally, a sudden change in the *CTE* indicates that the conductor is operating at the KPT.

### 4.1 | Approximation of actual curve and theoretical curve

The theoretical curve that describes the conductor behaviour is calculated after data processing is carried out on the measured data. For this purpose, the theoretical and measured tension values at the same temperature are compared. The theoretical curve and the actual conductor curve are adjusted using the least-squares method.

The temperature range of the measured values varied between 0 and 35 °C. Figure 8 shows an example of the temperature interval of conductor 1. A range of measured values in the temperature interval of 10 °C can be observed. The theoretical and actual tension curves (measurements) in this interval are approximated using the least-squares method.

### 4.2 | Estimation of CTE

To characterise the tension-temperature behaviour, the *CTE* is estimated for a temperature interval of 10 °C. The *CTE* corresponding to the conductor behaviour is calculated throughout this ten-degree temperature interval; the temperature is increased in steps of 1 °C within this interval, and the change in *CTE* is observed for each temperature.

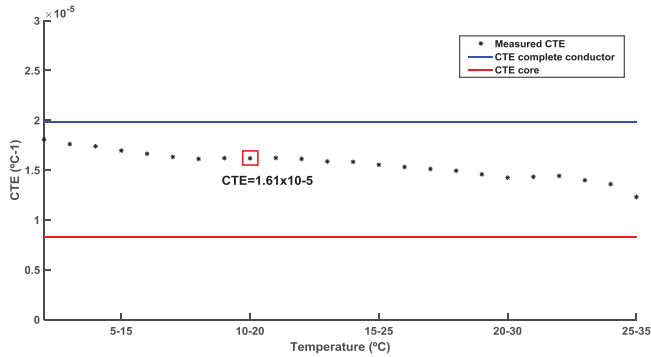


**FIGURE 9** Comparison of measured CTE and theoretical values as a function of temperature for conductor 1

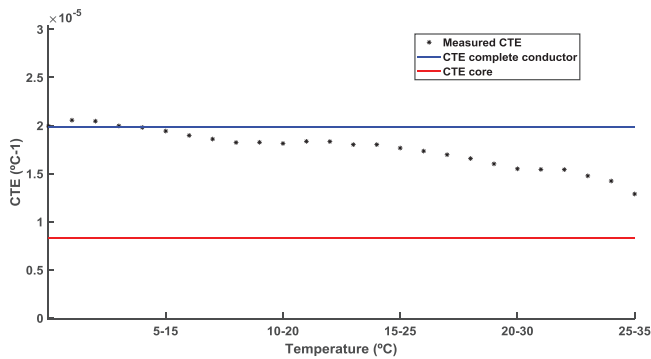


**FIGURE 10** Comparison of measured CTE and theoretical values as a function of temperature for conductor 2

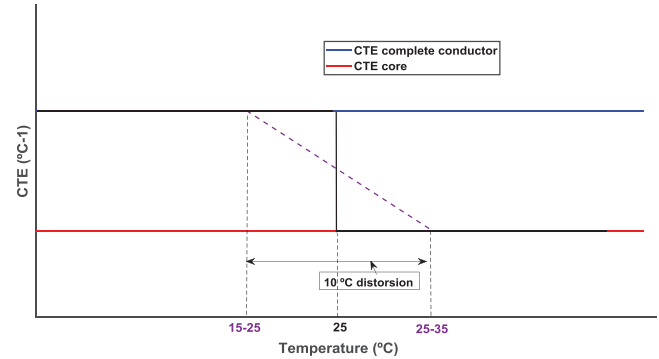
This process is repeated and the CTE estimation is carried out in the same way for subsequent 10 °C temperature intervals. Starting from 0 to 10 °C, the temperature is increased in each temperature interval until the last interval corresponding to 25–35 °C.

Figure 9 shows the CTE values obtained for conductor 1 and the CTE value obtained for the temperature range from 10 to 20 °C is highlighted by a red square.

Since the KPT in conductor 1 is the installation temperature (7 °C), Figure 9 shows that the behaviour of the conductor CTE is almost as expected below this temperature. But the expected change in CTE change at the KPT (7 °C) is not observed. As observed from the obtained data, the change in CTE, instead of being an abrupt change at a certain temperature, is rather a gradual one around the theoretical KPT.

Figure 10 shows the results obtained for conductor 2. The KPT measured during installation is 20 °C for conductor 2. Figure 10 shows that conductor 2 demonstrates the expected conductor CTE behaviour (complete conductor CTE) below the KPT. Similar to the case of conductor 1, no sudden change in the CTE was detected at the KPT. However, a gradual change was observed near the theoretical KPT. The measured CTE curve tends to reach the theoretical curve corresponding to the CTE behaviour of the core.

The CTE estimated through the CTE evaluation methodology produces distortion in the result. However, a gradual change



**FIGURE 11** CTE evolution conductor 1

in the CTE of the complete conductor and core is observed in the graph. This is due to the overlapping of temperatures in the 10 °C intervals in which the CTE estimation is performed.

Figure 11 shows an example of a conductor with a KPT of 25 °C. The black line shows the abrupt change from the CTE of complete conductor CTE to that of the core at a KPT of 25 °C. The purple dashed line represents the behaviour of the CTE estimated using the CTE evaluation methodology. It shows a gradual change from the CTE of the complete conductor to that of the core in the 10 °C interval.

Figure 11 shows a distortion of 10 °C in the result, which corresponds to 5 °C on either side of the KPT, produced by the CTE evaluation methodology. This distortion must be considered while analysing the result.

In the methodology, selecting a smaller interval would result in fewer data. Conversely, a larger interval, despite having large measurement data due to the total temperature range, limits the analysis since the distortion in the KPT range would be large. For this reason, 10 °C intervals were selected. Due to the selection of 10 °C intervals, a balance between the range used for the analysis and the minimum distortion in the results was achieved.

## 5 | RESULTS

From Figures 9 and 10, it can be seen that the KPT is in the form of a temperature range instead of being a specific temperature.

The results are plotted to obtain the curve shown in Figure 12. The curve shows a progressive change in the CTE of conductor 1 (purple curve).

By observing this progressive change in the CTE curve, the temperature at which the CTE would reach the theoretical value of the core CTE is estimated to be 55 °C. The interval corresponding to the change from complete conductor CTE to core CTE would be between 0 and 55 °C.

However, taking the distortion of 10 °C due to the CTE evaluation methodology into account, the temperature interval in which the gradual change from complete conductor CTE to core CTE occurs corresponds to the interval between 5 and 50 °C, that is, from the moment the aluminium starts to get slack at 5 °C until it gets slack at 50 °C. Therefore, the process would

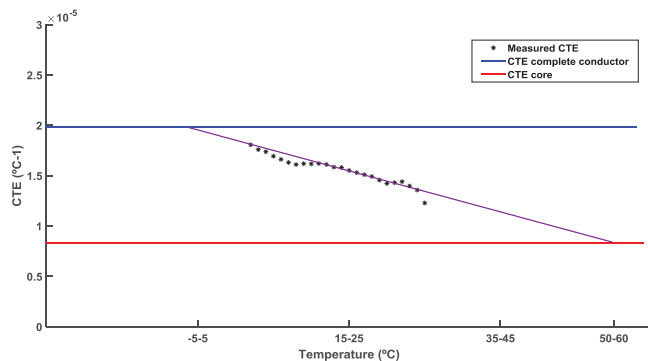


FIGURE 12 CTE evolution in conductor 1

require a 45 °C interval. In this case, if the KPT corresponded to the temperature at which an abrupt change in the CTE was observed, that KPT would have a displacement of 22.5 °C, that is, half of 45 °C.

Taking into account that the onset of CTE change began at 5 °C and considering the hypothesis suggesting an offset of 22.5 °C for the KPT, the KPT would be reached at 27.5 °C.

This offset or displacement estimated in KPT could be due to the possible compression value considered in the behaviour of the conductor. Researchers have calculated the compression value corresponding to this KPT offset as 9 MPa.

According to studies carried out in the literature in [21, 22], the authors determined that aluminium experiences compression before it gets slack, and a compression value around 10 MPa is considered while evaluating the behaviour of conductors. This compression value is close to the value observed from the results in the monitored line.

Hence, because of this effect, the KPT at which the aluminium gets slack is increased. Moreover, the graphical method implemented in commercial software programs such as SAG10 and PLS-CADD also considers the effects of compression. Both programs consider the KPT as the exact temperature at which the aluminium gets slack.

In [24], the authors discuss traditional models used to determine the mechanical behaviour of ACSR conductors, and the authors refer to the KPT as a temperature range instead of an exact temperature. Figure 12 shows that the change in CTE corresponding to an exact KPT is not abrupt but a gradual one.

Upon observing the results obtained from the monitored line, we obtained an offset for the KPT and a gradual change in the CTE corresponding to a range of temperatures that could be defined as the “KPT range”.

Figure 13 shows the evolution of sag in conductor 1 considering the KPT as the installation temperature 5 °C (purple line) and the evolution of sag if the KPT is 27.5 °C (red line). The sag evolution in the case of actual measurements is shown by the line with blue dots. It is observed that the actual measurements tend to reach the curve corresponding to the KPT of 27.5 °C at a value of around 50 °C. This is the temperature value estimated in the previous section on sag-temperature calculations in which the evolution of the CTE curve would reach the value of the CTE of the core.

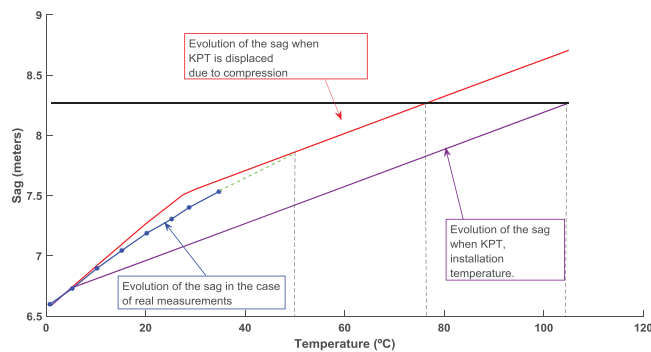


FIGURE 13 Sag versus temperature

It is observed from Figure 13 that if the KPT is 27.5 °C, the evolution of the sag curve reaches the maximum sag at 75.7 °C. In the design of the line, it is considered that the maximum sag of 8.26 m is reached at 105 °C; thus, the design has an error in the calculation of the maximum sag.

The ampacity limit of a conductor is related to the operating temperature and sag of the conductor. According to the static rating design at 105 °C, the maximum current that can flow without exceeding the maximum sag is 503.8 A, while at 75.7 °C, the ampacity is 397.1 A. This represents a 21% reduction in compared to the rated ampacity.

In other words, when the current is 503.8 A, the actual sag is higher than the expected 8.26 m. According to the results, the sag is 8.7 m.

The measurements recorded on the pilot line did not exceed 35 °C. However, they might increase since the CTE continues to gradually decrease with the increase in temperature until all the aluminium is slack.

## 6 | CONCLUSION

A gap-type conductor in operation was monitored to evaluate the KPT of the conductor. The KPT detection is based on the change in the conductor CTE values.

A novel procedure for CTE evaluation is proposed and verified. The proposed method fills the gap in the literature of methods that quantify the CTE and KPT from the line measurements in a systematic way. The CTE is estimated from the measured tension-temperature curve.

The CTE and KPT estimation procedure is applied in a pilot line. A new gap-type conductor was installed in the pilot line for line uprating purposes. The application of the method to a real line instead of a laboratory line allows characterizing the conductor in real working conditions.

Commercial sag-tension calculation software programs consider the effects of compression in the behaviour of the conductor, which results in an offset value for the KPT. However, the effects of compression are not considered in all cases. A KPT displacement was observed from the results obtained in this study. This is attributed to the compression value considered in the behaviour of the conductor. This performance aligns with

previous studies, which assumed that the aluminium is under compression before it gets slack. Further, the compression value corresponding to the KPT displacement calculated in this study agreed with the values presented in previous studies.

Usually, in sag-tension calculation methods, the change from complete conductor CTE to core CTE at KPT is considered to be abrupt. However, the results showed a gradual change in the CTE value. Therefore, the aluminium gets slack gradually. A gradual displacement in CTE was observed.

The KPT is a vital factor since it affects the sag of the conductor, which must be limited for safety reasons. Therefore, sag-tension calculation methods must consider the displacement in KPT and a gradual displacement in CTE. If these factors are neglected, there would be calculation errors in the temperature at which the maximum sag would be reached, and this would lead to a compromise in safety.

## ACKNOWLEDGEMENTS

This work is financially supported by the Ministerio de Economía, Industria y Competitividad, under the project DPI2016-77215-R (AEI/FEDER, UE) and by the University of the Basque Country UPV/EHU (ELEKTRIKER research group GIU20/034).

## CONFLICT OF INTEREST

The authors have declared no conflict of interest.

## ORCID

Miren T. Bedialauneta  <https://orcid.org/0000-0002-9392-6691>

Elvira Fernandez  <https://orcid.org/0000-0002-2667-5095>

Igor Albizu  <https://orcid.org/0000-0003-3475-5885>

A. Javier Mazon  <https://orcid.org/0000-0002-4572-4112>

## REFERENCES

1. CIGRE Brochure (Ref. No. 763): Conductors for the Uprating of Existing Overhead Lines (2019)
2. CIGRE Brochure 324: Sag-Tension Calculation Methods for Overhead Lines (2007)
3. Polevoy, A.: Impact of data errors on sag calculation accuracy for overhead transmission line. *IEEE Trans. Power Delivery* 29(5), 2040–2045 (2014)
4. Loudon, D., Douglass, D.A., Stephen, R.G., et al.: Calculation accuracy of high-temperature sag for ACSR in existing lines. *CIGRE Science & Engineering* 7 (2017)
5. Dong, X.: Analytic method to calculate and characterize the sag and tension of overhead lines. *IEEE Trans. Power Delivery* 31(5), 2064–2071 (2016).
6. Zein, H., Utami, S., et al.: Determination of overhead conductors curves with quadratic approach based. In: *International Conference on Technologies and Policies in Electric Power & Energy*, Yogyakarta, Indonesia, pp. 1–6 (2019)
7. Zhang, S.C., et al.: Power line simulation for safety distance detection using point clouds. *IEEE Access* 8, 165409–165418 (2020)
8. Zengin, A.T., et al.: Measurement of power line sagging using sensor data of a power line inspection robot. *IEEE Access* 8, 99198–99204 (2020).
9. Abbasi, M.Z., et al: Overhead transmission lines analysis considering sag-tension under maximum wind effect. *J. Mech. Continua Math. Sci.* 13(5), 185–192 (2018).
10. Omeje, C.O., Uahunmwangho, R.: Sag and tension evaluation of a 330 kV overhead transmission line network for upland and level land topographies. *Int. J. Sci. Eng. Res.* 11(3), 229–234 (2020)
11. Ahmad, A., et al.: Investigating tension in overhead high voltage power transmission line using finite element method. *Int. J. Electr. Power Energy Syst.* 114, 105418 (2020).
12. CIGRE Brochure (Ref. No. 353): Guidelines for increased utilization of existing overhead transmission lines (2008)
13. Riba, J.R., et al. : Uprating of transmission lines by means of HTLS conductors for a sustainable growth: Challenges, opportunities, and research needs. *Renewable Sustainable Energy Rev.* 134, 110334 (2020).
14. Fernandez, E., Albizu, I., Bedialauneta, M.T., et al.: Field validation of gap-type overhead conductor creep. *Int. J. Electr. Power Energy Syst.* 105, 602–611 (2019)
15. Yonezawa, K., Kinoshita, K.: Gap type conductor. *IEEE TP & C Line Design Meeting*, Las Vegas (2005)
16. CIGRE Brochure (Ref. No. 426): Guide for qualifying high temperature conductors for use on overhead transmission lines (2010)
17. Prasetyo, H. et al.: Analysis of knee point temperature (KPT) determination on high capacity low sag (HCLS) conductors for optimizing the ampacity load and sag on the overhead transmission lines system. *The 5th Annual Applied Science and Engineering Conference (AASEC 2020)*. In: *IOP Conference Series: Materials Science and Engineering*, p. 042021 (2021)
18. Pelacchi, P., Poli, D.: Thermo-mechanical model of multi-span overhead transmission lines equipped with high-temperature low-sag conductors. *Int. Rev. Modell. Simul.* 8(3), 331–338 (2015).
19. Bezerra, J.M.B., Silva, A.A.P., Lins, Z.D., et al.: Field validation of a new model for uprating transmission lines. *Electr. Power Syst. Res.* 134, 30–37 (2016).
20. Sibilant, G.C., Davidson, I.E., Stephen, R.G., et al.: Introduction to ACSR conductor sag at high temperature. *CIGRE-IEC Colloquium*, Montreal, Canada (2016)
21. Nigol, O., Barrett, J.S.: Characteristics of ACSR conductors at high temperatures and stresses. *IEEE Trans. Power Apparatus Syst.* PAS-100(2), 485–493 (1981).
22. Barrett, J.S., Dutta, S., Nigol, O.: A new computer model of ACSR conductors. *IEEE Trans. Power App. Syst.* PAS-102(3), 614–621 (1983).
23. Rawlins, C.B.: Some effects of mill practice on the stress strain behaviour of ACSR. *IEEE Trans. Power Delivery* 14(2), 602–629 (1999).
24. Mamala, A., Knych, T., Smyrak, B., et al.: An analytical model for the high temperature low sag conductor knee point determination. *Key Eng. Mater.* 641, 173–180 (2015)
25. Power Line Systems: PLS-CADD: Available from: [http://www.powline.com/products/pls\\_cadd.html](http://www.powline.com/products/pls_cadd.html). Accessed 15th May 2020
26. Southwire Company: SAG10: Available from: <https://overheadtransmission.southwire.com/sag10/>. Accessed 15th May 2020
27. Working Group SC 22-05 CIGRE: Permanent elongation of conductors. Predictor equations and evaluation methods. *Electra* 75, 63–98 (1981)
28. Kopsidas, K., Boumecid, B., Cooper, I.P.: Overhead line design considerations for conductor creep mitigation. *IET Gener. Transm. Distrib.* 10(10), 2424–2432 (2016)
29. Bedialauneta, M.T., Fernandez, E., Albizu, I., et al.: Factors that affect the sag-tension model of an overhead conductor. In: *2013 IEEE PowerTech Conference*, Grenoble, France, pp. 1–6 (2013)
30. Bedialauneta, M.T., Albizu, I., Fernandez, E., et al.: Uncertainties in the testing of the coefficient of thermal expansion of overhead conductors. *Energies* 13(2), 411 (2020)
31. EN 50182: Conductors for overhead lines - Round wire concentric lay stranded conductors (2001)
32. IEC 62420: Concentric lay stranded overhead electrical conductors containing one or more gap(s) (2008)
33. EN 50540: Conductors for overhead lines - Aluminium Conductors Steel Supported (ACSS) (2010)

**How to cite this article:** Bedialauneta, M.T., et al.: Sag-tension evaluation of high-temperature gap-type conductor in operation. *IET Gener. Transm. Distrib.* 16, 19–26 (2022). <https://doi.org/10.1049/gtd2.12288>